Available online at www.sciencedirect.com
SCIENCE DIRECT
Journal of Power Sources 146 (2005) 335–339
JOURNAL OF POWER SOURCES
www.elsevier.com/locate/jpowsour

Stable-cycle and high-capacity conductive sulfur-containing cathode materials for rechargeable lithium batteries

Xianguo Yu *, Jingying Xie, Ying Li, Haijiang Huang, Chunyan Lai, Ke Wang

Energy Science and Technology Laboratory, Shanghai Institute of Microsystem and Information Technology, Chinese Academy of Sciences, Shanghai 200050, China

Available online 27 July 2005

Abstract

Cycle characteristics of conductive sulfur-containing materials (CSMs) synthesized by heating the mixture of polyacrylonitrile and elemental sulfur at a wider temperature region from 250 to 800 °C are presented. The cyclability is improved remarkably for CSMs obtained above 400 °C. A stable capacity of CSM prepared at 450 °C maintains about 470 mAh g^{-1} and the capacity retention remains ca. 90% after near 380 cycles. Fourier-transform infrared spectroscopy (FTIR) and Raman characterizations disclose that the fundamental chemical structure of CSMs is composed of dehydropyridine type matrix with S–S bond in side-chain. Such unique structure and better electrical conductivity ensure the excellent cycle performance of the prepared CSMs.

Keywords: Conductive polymer; Elemental sulfur; Cathode materials; Rechargeable lithium batteries

1. Introduction

It is generally known that lithium/sulfur batteries face serious problems of low active material utilization and cycle life [1–3]. The electrically and ionically nonconductive nature of sulfur, the solvent-solubility of polysulfide reaction products, and the incomplete reversibility of lower-order sulfides as well as the degradation of lithium anode are responsible for the deterioration of cycle life. Control of rapid capacity fade and improvement of active-material utilization are vital for its real applications. Many attempts, including addition of conductive additives in cathode [4], selection of proper electrolytes [5], employment of all-solid-state polymer electrolytes [6], and surface modification of lithium anode [7], etc. have been carried out to improve cycle life of Li/S batteries. For example, electron conducting polymers [8] and porous active carbon [9] have also been incorporated with elemental sulfur to enhance conductivity and to improve dispersed state of sulfur. However, the capacity reduction for the reported Li/S batteries still remains fast relatively.

Recently, our research group have selected polyacrlyonitrile (PAN) as the reaction precursor to co-heat with elemental sulfur at 280–300 °C, obtaining a novel conductive sulfur-containing material (CSM). Its reversible capacity reaches ca. 600 mAh g^{-1} and the capacity fade rate is about 26% after 50 cycles in cells with gel-type polymer electrolyte, improving the charge-discharge performance of sulfur-containing material to a great extent [10–11]. When evaluated in all-solid-state polymer cells with PEO-based electrolytes, the CSM exhibits slightly improved cyclability while the capacity becomes lower [12]. In the present paper, various CSM samples are prepared under different synthesis temperatures. The improvement of long-life cycle performance for CSMs obtained at relatively higher temperatures is emphasized. Meanwhile, causes for such an improvement of cycle performance are analyzed preliminarily.

2. Experimental

2.1. Material preparation and characterization

At a wider temperature range of 250–800 °C, various CSM samples were synthesized as described previously [10].

* Corresponding author. Tel.: +86 21 62131647; fax: +86 21 62131647.
E-mail address: yuxg@mail.sim.ac.cn (X. Yu).

0378-7753/$ – see front matter © 2005 Elsevier B.V. All rights reserved.
doi:10.1016/j.jpowsour.2005.03.021

The temperature-rising rate and reaction soak time were fixed as 10 °C min^{-1} and 8 h, respectively. The samples have been endowed with markers. For example, CSM-500 designates the CSM synthesized at 500 °C. For comparison, the pyrolysates of PAN at corresponding temperatures were also prepared. Scanning electron microscope (SEM) was performed in a JEOL Model JSM-5300 apparatus. Fourier-transform infrared spectroscopy (FTIR) data were recorded from pellets of CSM mixing KBr on a Perkin-Elmer (L-710) spectrophotometer. Raman spectra were carried out on a Lab Ram1B system with a He–Ne lamp-house, whose wavelength is 632.8 nm.

2.2. Electrode fabrication and electrochemical tests

Seventy weight percent CSM active material, 20 wt.% acetylene black (AB) and 10 wt.% poly-tetrafluorethylene (PTFE) binder were homogenously mixed in ethanol under magnetic stirring. The produced paste after ethanol dispersant evaporation was shaped into a thin self-sustainable film and then it was dried under vacuum at 80 °C for 6 h. The dried film with thickness ca. 70–80 μm was incised into pellets with diameter of 10 mm, and then they were pressed onto a foamed nickel current collector to form positive electrodes. The loaded active material of CSM was about 4.5 mg. Electrochemical properties of CSM were evaluated via CR2025-type coin cells containing 1 M $LiPF_6$/ethylene carbonate (EC) + dimethyl carbonate (DMC) (1:1 in volume) electrolyte. A lithium sheet acted as the counter electrode. Celgard2300 porous film was used as separator. Unless stated otherwise, charge and discharge current density were 0.2 mA cm^{-2} and voltage cutoff was controlled between 3.0 and 1.0 V versus Li/Li$^+$. The calculation of specific capacity for each sample was based on the loaded active material.

3. Results and discussion

The cycle characteristics of CSMs prepared at different temperatures from the second cycle are shown in Fig. 1. It is clear that cyclability behaviors for CSMs obtained at/below 350 °C are different from those for ones synthesized at/above 450 °C. CSM-300 presents the highest capacity in the initial several decade cycles, but the capacity falls dramatically. CSM-350 shows a mildly capacity reduction. For CSMs synthesized at 400–500 °C, the cyclability is greatly improved with a certain loss of capacity. The 2nd, 50th and 380th specific capacity for CSM-450 are ca. 520, 503 and 470 mAh g^{-1}, respectively, and the capacity retention remains about 90% after 380 cycles based on the second discharge capacity. The cycle stability is further improved while the capacity drops as increasing synthesis temperature again. Interestingly, different from CSMs synthesized below 500 °C, there seems an active process for those synthesized at/over 500 °C, e.g., the capacity increases gradually from ca. 100 mAh g^{-1} in the second cycle to more than 140 mAh g^{-1} after 400 cycles for CSM-800.

The temperature dependence of cycle behaviors relates to the change of the composition and structure of CSM. Nano-sulfur, embedded in a thermally stable heterocyclic compound formed by the dehydrogenating and cycling of PAN, was regarded as electrochemical active component [11]. However, despite at the nano-sized, elemental sulfur inevitably exhibits relatively fast capacity reduction, suggesting the reversible capacity for CSMs mainly derives from the electrochemical redox of organosulfide-like disulfur bonds. Fig. 2 shows the FTIR spectra of CSMs and of PAN pyrolysates. According to the skeletal vibrations for pyrolysate of PAN, pyridine and pyrrole [13,14], the group of peaks at the region of 1600–1200 cm^{-1} and the characteristic peak at 802 cm^{-1} indicate the formation of π-conjugated co-plane hexahydric-ring containing C=C and C=N bonds. The π-conjugated electrons favor the electrical conduction of CSMs and such conduction will be facilitated with the intermolecular cross-link and denitrogenation when increasing

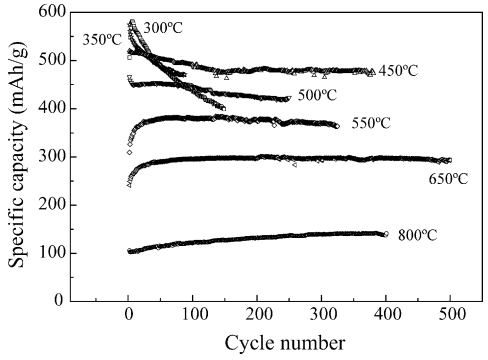

Fig. 1. Variation of the discharge capacity as a function of cycle number from the second cycle for CSMs synthesized at different temperatures.

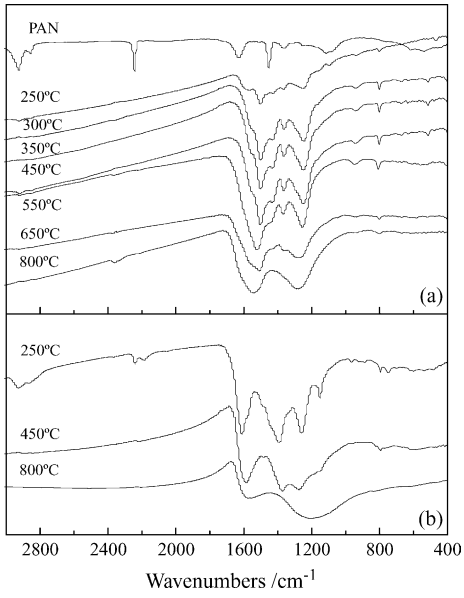

Fig. 2. FTIR spectra of (a) PAN and CSMs prepared at different temperatures; (b) pyrolysates of PAN at selected temperatures.

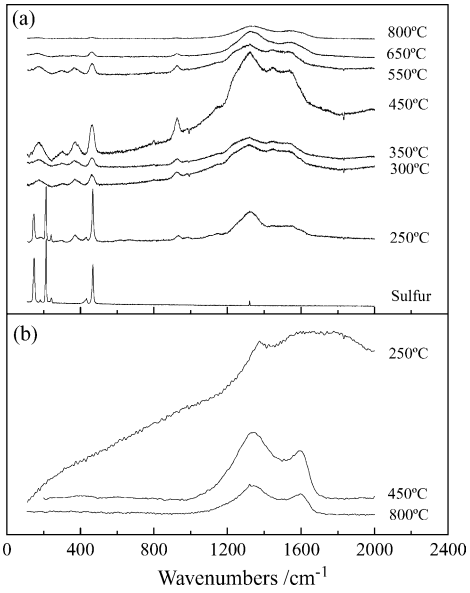

Fig. 3. Raman shifts of (a) CSMs and sulfur; (b) pyrolysates of PAN.

synthesis temperature. Peaks at ca. 943, 670 and at 513 cm^{-1} come forth, although they are very weak. Those peaks are characteristic for CSMs because they do not appear in the FTIR spectra of either the pyrolysates of PAN or elemental sulfur. The peak at 513 cm^{-1} can be ascribed to the S–S stretch, based on assignments for organodisulfides [15]. We assign the peak at 943 cm^{-1} to ring breath, in which C–S bond is contained, and 670 cm^{-1} to C–S stretch [16–18]. The C–S and S–S peaks for CSM-650 and CSM-800 are very weak.

The existences of S–S bond and C–S bond have also been affirmed by Raman spectra in Fig. 3. The three strong peaks at ca 217, 150 and 471 cm^{-1} for elemental sulfur disappear in the spectra for CSMs prepared above 300 °C. And also, peaks located at 305, 374, 460, 927 and 1142 cm^{-1}, which do not appear in the spectrum of pyrolysate of pure PAN, come forth, further indicating chemical reactions have occurred between elemental sulfur and matrix of cyclized PAN. Therefore a ring, containing such covalent bonds as –C–S–S–C–, has formed at the side-chain of the cyclized PAN. The electrochemical cleavage of such sulfur–sulfur bond during discharge does not cause the depolymerization of CSMs and thus the Li-insertion reduction product shows almost non-solubility in solvent.

Morphologically, there are almost no evident differences among CSMs and they present as submicron or nano-sized spherical particles with average diameter of ca. 250 nm as shown in Fig. 4. However, the electron transfer and lithium diffusion may be different. CSMs possess a disordered layer stacking phase structure, similar to that of amorphous carbon and trace nano-sulfur inserts into the gap of neighbor crystallites or in nano-pores at a relatively low synthesis temperature [19]. In this case, the obstacle of charge transfer in particles owing to the lower conductivity is one of the reasons for the rapid capacity fade of CSMs-300 and CSMs-350. For

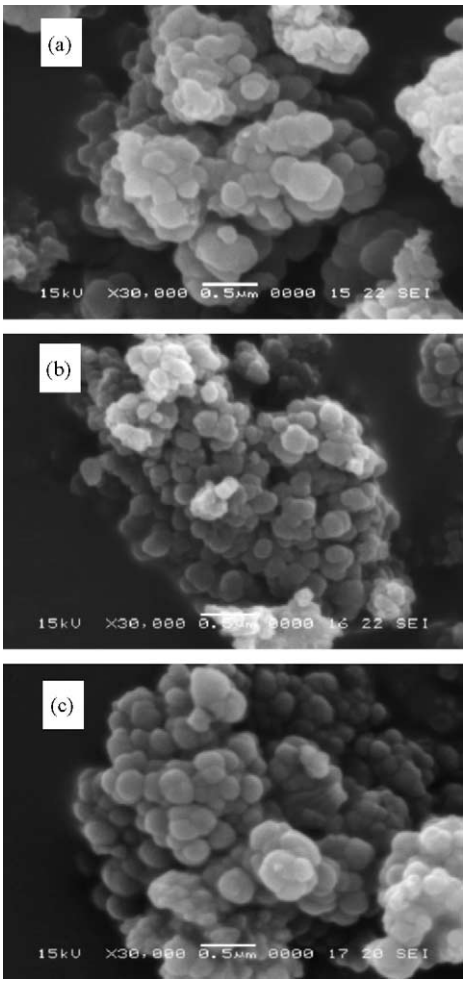

Fig. 4. SEM images for the samples of (a) CSM-300; (b) CSM-450; (c) CSM-800.

samples obtained above 500 °C, relatively higher electrical conductivity makes charge transfer easy in fine particles in spite of the severe particle aggregation, while lithium solid-diffusion may become predominant limitation. The reversible capacity increases in the initial stage for CSM-550 and CSM-650 (Fig. 1). It means that the active functional group of disulfur bond is not completely utilized at the beginning.

The polarizability of the charge-discharge curves of CSMs presented in Fig. 5 can also be, to some extent, used to character electrochemical kinetics. For the samples prepared below 500 °C, the mild increase of average plateau voltage for Li-insertion and the slight decrease of that for Li-extraction from the second cycle indicate the kinetic resistance of the electrochemical reaction between active sulfur and lithium has abated, which can be attributed to the progressive enhancement of electrical conductivity of CSMs as raising preparation temperature. For the samples prepared above 500 °C, electrical conductivity probably already reaches a certain high value accompanied with the carbonization and desulfurization of CSMs. On the other hand, the increase of carbonization and decrease of sulfur

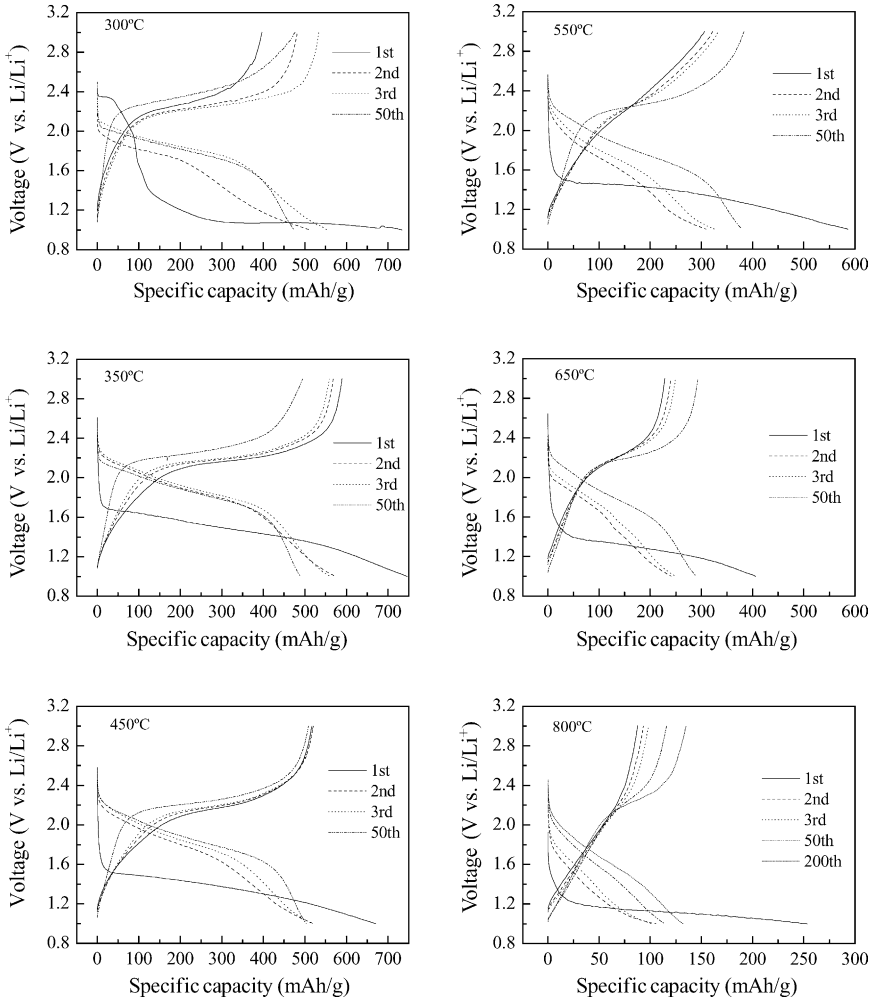

Fig. 5. Charge and discharge profiles of the corresponding CSMs.

content cause that part of active sulfur is enveloped deeply within the amorphous carbon-like structure. Thus, lithium access to the surface of active sulfur is blocked and only after activation with longer cycles can active sulfur work normally again. The discrepancies among the initial discharge processes of CSMs are also obvious. The voltage that lithium begins to intercalate into CSM for the first discharge descends gradually as the increase of synthesis temperature. A relatively high voltage plateau at ca. 2.36 V for CSM-300 are found, which corresponds to the reduction of elemental sulfur. But there is almost no capacity contribution until the voltage drops to ca. 1.2 V for CSM-800. In summary, the unique molecular structure of dehydropyridine type matrix with S–S bond in side-chain and the improvement of electrical conductivity justify the excellent cycle performance for higher temperature prepared CSMs.

4. Conclusions

The cyclability and capacity of the co-heating product of polyacrylonitrile and elemental sulfur depend primarily on synthesis temperature. CSM-250 is unable to be charged and discharged in lithium cells. CSM-300 and CSM-350 possess high capacity, while their capacity fade rates are fast. In contrast with these lower temperature prepared samples, those obtained at higher temperatures of 550–800 °C exhibit excellent cyclic stability, but the capacity is rather low. In view of excellent cyclability and high capacity, the optimization synthesis temperature range appears to be from 450 to 500 °C. A stable cyclic capacity of ca. 470 mAh g^{-1} over 380 cycles displays great potential for CSM to be used as high performance cathode material in rechargeable lithium batteries. The excellent cyclability of CSMs results from the special molecular structure of CSMs and the higher electrical conductivity.

References

[1] H. Yamin, A. Gorenshtein, J. Penciner, Y. Sternberg, E. Peled, J. Electrochem. Soc. 135 (1988) 1045.
[2] E. Peled, T. Sternberg, A. Gorenshtein, Y. Lavi, J. Electrochem. Soc. 136 (1989) 1621.

[3] E. Peled, A. Gorenshtein, M. Segal, Y. Sternberg, J. Power Sources 26 (1989) 269.
[4] S.-C. Han, M.-S. Song, H. Lee, H.-S. Kim, H.-J. Ahn, J.-Y. Lee, J. Electrochem. Soc. 150 (2003) A889.
[5] D. Marmorstein, T.H. Yu, K.A. Striebel, F.R. Mclarnon, J. Hou, E.J. Cairns, J. Power Sources 89 (2000) 219.
[6] J.H. Shin, K.W. Kim, H.J. Ahn, J.H. Ahn, Mater. Sci. Eng. B95 (2002) 148.
[7] Y.M. Lee, N.-S. Choi, J.H. Park, J.-K. Park, J. Power Sources 119–121 (2003) 964.
[8] A. Perichand, L. Mehaute, US Patent US4664991 (1987).
[9] J.L. Wang, J. Yang, J.Y. Xie, N.X. Xu, Y. Li, Electrochem. Commun. 4 (2002) 499.
[10] J.L. Wang, J. Yang, J.Y. Xie, N.X. Xu, Adv. Mater. 14 (2002) 963.
[11] J.L. Wang, J. Yang, C.R. Wan, K. Du, J.Y. Xie, N.X. Xu, Adv. Funct. Mater. 13 (2003) 487.
[12] X.G. Yu, J.Y. Xie, J. Yang, K. Wang, J. Power Sources 132 (2004) 181.
[13] K. Jobst, L. Sawtschenko, M. Schwarzenberg, L. Wuckel, Synth. Met. 47 (1992) 279.
[14] D. Lin-Vien, N.B. Colthrup, W.G. Fateley, J.G. Grasselli, The Handbook of Infrared and Raman Characteristic Frequencies of Organic Molecules, Academic Press, San Diego, CA, 1991.
[15] J.M. Pope, T. Sato, E. Shoji, D.A. Buttry, T. Sotomura, N. Oyama, J. Power Sources 68 (1997) 739.
[16] J.M. Pope, T. Sato, E. Shoji, N. Oyama, K.C. White, D.A. Buttry, J. Electrochem. Soc. 149 (2002) A939.
[17] N.B. Colthup, L.H. Daly, S.E. Wiberley, Introduction to Infrared and Raman Spectroscopy, Academic Press, San Diego, CA, 1990.
[18] L.J. Xue, J.X. Li, S.Q. Hu, M.X. Zhang, Y.H. Zhou, C.M. Zhan, Electrochem. Commun. 5 (2003) 903.
[19] X.G. Yu, J.Y. Xie, J. Yang, H.J. Huang, K. Wang, J. Electroanal. Chem. 573 (2004) 121–128.